

14 **Abstract**

15 The invasion of dreissenid mussels has profoundly altered benthic physical environments
16 and whole-lake nutrient cycling in the Great Lakes over the past several decades. The
17 resurgence of the filamentous green alga *Cladophora* appears to be one of the consequences
18 of this invasion. Sloughed *Cladophora* deteriorates water quality, fouls recreational beaches,
19 and may contribute to outbreaks of avian botulism, which have been especially severe in the
20 Sleeping Bear Dunes National Lakeshore (SLBE) region of Lake Michigan. To help
21 determine the fate of sloughed *Cladophora*, a Lagrangian particle trajectory model was
22 developed to track the transport of *Cladophora* fragments in the nearshore zone based upon a
23 physical transport-mixing model. The model results demonstrate that the primary deposition
24 sites of sloughed *Cladophora* within the SLBE region are mid-depth sites not far away from
25 their initial growth area. Because of high algae production in the nearshore waters and limited
26 exchange between the inner and outer bay, the shoreline beach of Platte Bay appears to be
27 particularly vulnerable to fouling, with overall three times as many accumulated particles as
28 those along the Sleeping Bear Bay and Good Harbor Bay. The results of this model may be
29 used to guide regional environmental management initiatives and provide insights into the
30 mechanisms responsible for avian botulism outbreaks. This model may also inform the
31 development of whole-lake ecosystem models that account for nearshore-offshore
32 interactions.

33

34

35

36

37

38 **Keywords:** *Cladophora*, ecosystem health, numerical modelling, Lake Michigan, national
39 lakeshore, hydrodynamics.

40

41 **Introduction**

42 *Cladophora* is a filamentous green alga that has frequently grown at nuisance levels in the
43 nearshore zone of the Laurentian Great Lakes since the 1950s as a result of lake-wide
44 eutrophication (Auer et al., 2010; Higgins et al., 2005a). This alga primarily grows on hard
45 substrate in the nearshore zone (<30 m depth) where its growth may be limited by light and/or
46 nutrients (Dayton et al., 2014; Bootsma et al., 2015; Gill et al., 2018). Recent studies in Lake
47 Erie revealed a surprisingly high-coverage as much as 40% of the nearshore benthic area
48 during productive seasons (Brooks et al., 2015). The implementation of phosphorus
49 management programs during the late 1970s successfully led to significant reductions of
50 *Cladophora* biomass in the Great Lakes (Bootsma and Liao, 2013; Chapra and Sonzogni,
51 1979). However, the establishment of dense populations of dreissenid mussels in the Great
52 Lakes has altered physical and biogeochemical conditions in such a way as to favor
53 *Cladophora* growth, despite the declines in phosphorus loading that have been achieved over
54 the past five decades. Nearshore waters have become clearer, due to plankton reductions
55 resulting from mussel grazing, resulting in higher depth-specific growth rates of benthic algae,
56 and extension of the depth range over which benthic algae can grow (Auer et al., 2010).
57 Hecky et al. (2004) suggested that dreissenid grazing would result in more efficient retention
58 of phosphorus in the nearshore zone, and radionuclide tracer studies support this hypothesis,
59 showing that nearshore dreissenids rely heavily on plankton transported from the pelagic to
60 the nearshore (Waples et al., 2017). Recycling of nutrients in this food source by nearshore
61 dreissenids results in a supply of dissolved phosphorus that is directly available to benthic
62 algae growing adjacent to dreissenids (Bootsma and Liao 2013; Dayton et al. 2014). Creation
63 of hard benthic substrate in the form of dreissenid shells may also provide greater benthic
64 surface areas on which *Cladophora* can grow (Higgins et al., 2008). As a result of these
65 various factors, *Cladophora* biomass is now comparable to that during the peak
66 eutrophication period (Bootsma et al., 2004; Tomlinson et al., 2010).

67 The resurgence of *Cladophora* has had numerous ecological and economic effects. A
68 significant portion of sloughed *Cladophora* is ultimately stranded on shore, where it
69 negatively affects aesthetic conditions, tourism, and the value of lakeshore property
70 (Kuczynski et al., 2016; Lenzi et al., 2015). Stranded *Cladophora* can also facilitate the

71 persistence of enteric bacteria and other human pathogens, resulting in health risks (Chun et
72 al., 2017; Przybyla-Kelly et al., 2013). Within the lake, bacterial decomposition of decaying
73 mats of *Cladophora* can result in near-bottom hypoxic and anoxic conditions (Tyner, 2013),
74 which will alter the abundance and composition of benthic invertebrates and may promote the
75 growth of the bacterium *Clostridium botulinum* and the production of the botulism neurotoxin
76 (Chun et al., 2013; Mathai et al., 2019), which has resulted in the deaths of thousands of birds
77 in the Sleeping Bear Dunes National Lakeshore region in some years (Chun et al., 2013;
78 Princé et al., 2017). Hence, an understanding of the mechanisms regulating the sloughing,
79 transport, and deposition of *Cladophora* may improve our understanding of the conditions
80 that lead to avian botulism outbreaks, and our ability to predict these outbreaks.

81 Numerical models are useful tools to reproduce the spatiotemporal dynamics of the
82 lake-wide ecosystem, and to explore the underlying mechanisms that control these dynamics.
83 A number of modelling studies have been conducted in the Great Lakes to explore a variety of
84 physical, biological and ecological processes, including mass transport (Bai et al., 2013;
85 Beletsky et al., 2013), nutrient cycling (Chen et al., 2002), and invasive dreissenid impacts
86 (Rowe et al., 2017; Shen et al., 2018). Several models have been used simulate *Cladophora*
87 growth and biomass, which is primarily driven by solar radiation, water temperature, and
88 soluble reactive phosphorus (Higgins et al., 2005b; Tomlinson et al., 2010; Auer et al., 2021).
89 Higgins et al. (2005b) simulated *Cladophora* sloughing as a function of wave-induced shear
90 stress, which was modified by Malkin et al. (2008) to include “catastrophic detachment”
91 under conditions of high winds, high waves, and high *Cladophora* biomass. By comparison,
92 the transport and fate of *Cladophora* after sloughing has received little attention, despite the
93 fact that these processes likely play a critical role in determining the impacts of excessive
94 *Cladophora* growth on human activities and important ecosystem processes such as nutrient
95 and energy transport (e.g., Turschak et al., 2014), oxygen consumption, and the growth of
96 potentially toxic bacteria.

97 In this study, we constructed a 3-D hydrodynamic model of Lake Michigan to reproduce
98 multiple physical processes. Simulation results were validated against empirical observations.
99 A Lagrangian particle trajectory model was embedded in the whole-lake model to track the
100 transport of detached *Cladophora* mats within the Sleeping Bear Dunes National Lakeshore

101 area based upon the physical model outputs. Our goal was to identify potential hotspots where
102 sloughed *Cladophora* mats are likely to accumulate within the lake, and to identify the
103 pathways between *Cladophora* sloughing and stranding along the shoreline beaches. A
104 longer-term goal is to incorporate this *Cladophora* transport model into a broader
105 whole-lake-wide physical-biogeochemical model to better understand nearshore-offshore
106 interactions.

107

108 **Materials and Methods**

109 **Study Site**

110 Sleeping Bear Dunes National Lakeshore (SLBE) is located along the northwest coast of
111 Michigan's lower peninsula (Fig. 1a). It is the second most-visited of the Great Lakes national
112 parks with more than a million visitors per year. The coastal region of the national lakeshore
113 is characterized by a complex bathymetry covering a wide range of depths from 5 m to 150 m
114 (Fig. 1b). The lake bottom is a mix of hard (rocky) and soft (sand, silt) substrate. Hard
115 substrate is densely covered with quagga mussels, and at depths less than ~15 m hard
116 substrate is also covered with dense benthic algal growth from late May until
117 September/October. Mussel and benthic algae abundance, along with other environmental
118 variables, have been monitored at a long-term research site in Good Harbor Bay since 2010,
119 where the substrate is primarily rocky. Mean mussel density at this site is 4,000 to 5,000/m²,
120 and benthic algal biomass, which is dominated by *Cladophora* for most of the summer,
121 usually peaks at between 100 and 200 g dry weight per m². Fouling of local beaches with
122 sloughed *Cladophora* is common on both the mainland and islands, primarily from
123 mid-summer to fall, and these decomposing algae may promote the growth of *Clostridium*
124 *botulinum* (Byappanahalli and Whitman, 2009). Bird deaths due to avian botulism are
125 especially frequent in this part of Lake Michigan (Chipault et al., 2015).

126

127 **Hydrodynamic Model**

128 The hydrodynamic circulation and mixing model used in this study is the Finite Volume
129 Community Ocean Model (FVCOM). The model has been adapted and used for the Great
130 Lakes, and has been shown to reliably reproduce regional and lake-wide physical dynamics at
131 various time scales (Anderson et al., 2015; Rowe et al., 2016; Xue et al., 2015). The

132 horizontal unstructured mesh in this study contains 3301 nodes and 6242 triangle elements,
133 with higher resolution in the nearshore (~1.2 km between nodes on average) compared with
134 the offshore (~3.5 km, Fig.1). A sigma coordinate was used in the vertical direction (30 layers)
135 with higher resolution approaching the surface and bottom to better resolve mixing processes
136 near the boundaries. Other model configurations include a roughness height of 0.5 mm for a
137 logarithmic bottom boundary layer, 2.5 level Mellor-Yamada turbulence closure scheme for
138 vertical mixing, and the formulation of Smagorinsky for horizontal diffusion. The background
139 diffusivity and viscosity were set at $1 \times 10^{-6} \text{ m}^2 \text{ s}^{-1}$. The model boundary was closed at the
140 Straits of Mackinac which connects Lake Michigan and Lake Huron. Surrounding tributaries
141 were not included as they are expected to have a negligible effect on whole-lake circulation.
142 In this study, we hindcasted the hydrodynamic conditions for 2013. Lake-wide simulations
143 were initiated on March 1st with a spatially uniform water temperature of 4.0 °C, and were
144 run for 9 months until the end of November. The first 30 days are considered as model
145 spin-up to obtain a hot-start with ambient flow, water temperature and surface elevations. A
146 mode split technique, which separates vertical integration equations from vertical structure
147 equations, was applied within FVCOM for better computing efficiency. The time step of the
148 external mode (integrated equations) was set to 10 s to avoid advective instability according
149 to the Courant-Friedrich Levy (CFL) criterion, and the split number was set to 10, which
150 represents a time step of 100 s for the internal mode (structure equations).

151

152 **Lagrangian Particle Trajectory Model**

153 We constructed a 3-D Lagrangian particle trajectory model following the procedures
154 described by Beletsky et al. (2007) based on a new Matlab platform featured with flexible
155 postprocess and explicit visualization. The advection of particles was determined as:

$$156 \quad \frac{dx}{dt} = u(x, y, z), \quad \frac{dy}{dt} = v(x, y, z), \quad \frac{dz}{dt} = w(x, y, z)$$

157 (1)

158 where x , y , z are the positions of the particle, and u , v , w are the velocity components. A
159 higher resolution unstructured mesh (~100m, Fig.1b) for the SLBE lakeshore region was
160 nested into the large lake-wide mesh to precisely track the motions of *Cladophora* ‘particles’.
161 The velocity components with higher spatiotemporal resolutions for the SLBE lakeshore area

162 were linearly interpolated from the whole-lake FVCOM outputs. The motion of particles due
163 to physical advection was updated by integrating Eq.1 using an explicit fourth-order
164 Runge-Kutta scheme with a time step of 300 s (5 min). Turbulence eddy diffusivity induced
165 vertical mixing movement was calculated using the random walking scheme from Huret et al.
166 (2007),

$$167 \quad z(t + \delta t) = z(t) + w_b \delta t + K'(z(t))\delta t + R \sqrt{\frac{2K(\bar{z})\delta t}{\sigma^2}} \quad (2)$$

168 in which, δt is the vertical random walk time step (set as 10 s), w_b is the sinking velocity,
169 K is the vertical diffusivity, K' is the diffusivity gradient, R is a random variable from a
170 distribution with zero mean and standard deviation of σ , and $\bar{z} = z + 0.5K'\delta t$. Particle
171 transport across the surface and bottom boundaries was not permitted, and the *Cladophora*
172 particles were assumed to stay at the shoreline if they reached the lake-land boundary. The
173 sinking velocity was set as 10 m day⁻¹ according to Rowe et al. (2016). The current speed of
174 resuspension threshold for deposited particles was set as 2 cm s⁻¹ according to the laboratory
175 experiments (Flindt et al., 2007).

176 The Lagrangian particle trajectory model was run for 3 months from June to August,
177 2013 to track the transport of sloughed *Cladophora* from a simplified perspective. 200
178 particles were initially released at the shallow nearshore area (<10 m) along the shoreline and
179 islands at the beginning of June (Fig. 2), and an extra of 200 particles were released every 5
180 days assuming a constant sloughing rate until the end of summer when growth slows.
181 Released particles were all initially distributed at the middle position of the water column.

182

183 **Model Forcing and Field Data**

184 The bathymetry of Lake Michigan including the SLBE coastal area was obtained from
185 the NOAA National Geophysical Data Center
186 (<https://www.ngdc.noaa.gov/mgg/greatlakes/michigan.html>) with ~2 km resolution for open
187 lake and ~400 m for nearshore waters. The bathymetry data was interpolated into the mesh
188 grids based on a natural neighbor interpolation algorithm for further model setup. The
189 hydrodynamic model FVCOM was forced by surface heat radiation flux and air-sea
190 momentum as driven by meteorological conditions including wind speed at a height of 10 m,

191 short wave radiation, relative humidity, cloud cover and air temperature following the
192 methods from Beletsky and Schwab (2001). These meteorological data were directly
193 downloaded from the North American Regional Reanalysis (NARR) database which is a
194 32-km-resolution and 3-hr interval dataset
195 (psl.noaa.gov/data/gridded/data.narr.monolevel.html) and is derived from the NCEP
196 meteorological model with assimilation of observational data from variable sources including
197 remoting sensing and the Great Lakes buoy data. Surface water temperature of Lake
198 Michigan was obtained from the Great Lakes Surface Environmental Analysis
199 (coastwatch.glerl.noaa.gov/glsea) based on satellite observations.

200 Field measurements were conducted at the Good Harbor Bay in 2013 to collect a time
201 series of *Cladophora* biomass. A bottom-mounted Acoustic Doppler Current Profiler (ADCP,
202 250 kHz) was deployed at a 10m-depth site of Good Harbor Bay (*Cladophora* producing site,
203 Fig. 2) from June to October, 2013 to collect the vertical profiles of the current velocity at
204 one-hour intervals with 1-meter vertical resolution. We also installed a camera with a vertical
205 measuring stick planted in a 20m-depth site for field view (*Cladophora* depositional area, Fig.
206 2), allowing us to monitor the thickness of the depositional bed over time (Fig. 3). While the
207 time lapse imagery does not allow for quantitative measurements of biomass as accurate as
208 those derived from grab samples, it allows for semi-quantitative measurements at high
209 temporal resolution (hourly daytime images), which allows for the identification of major
210 sloughing, resuspension, and depositional events.

211

212 **Results and Discussion**

213 **Physical results**

214 Simulated surface water temperatures in the SLBE nearshore region agreed reasonably
215 well with satellite observations, with an average root mean square error (RMSE) of 0.6 °C
216 over the year (Fig. 4). Seasonal dynamics of surface water temperature were captured well,
217 characterized by a gradual increase from early spring to a maximum in late July/early August,
218 and a gradual decrease through autumn. The model was able to capture the observed dramatic
219 temperature decline in mid-August, although it slightly overestimated the magnitude of the
220 decline. Discrepancies between simulations and observations in spring and early summer are

221 likely the result of the assumed spatially uniform initial conditions with barely one-month
222 spin-up.

223 The eastern (u) and northern (v) velocity components from the ADCP mounted at the
224 bottom of 10m-depth site (Fig. 2) were used to validate the near-bottom current simulations.
225 Comparison results indicated a satisfying performance of the physical model in reproducing
226 the current speed, particularly after late July (Fig. 4). In general, an average benthic current
227 speed of 1.4 cm s^{-1} was recorded by the ADCP over the summer, while the model predicted a
228 slightly higher value of 1.6 cm s^{-1} . The standard deviations of current variations, which are
229 likely due to basin scale waves, were 0.84 cm s^{-1} from model simulation, and 0.73 cm s^{-1} from
230 field observations. Compared to our previous simulations at a deeper, open-water site (55m,
231 Shen et al., 2020), it is more challenging to reproduce the hydrodynamic environment at
232 shallow nearshore regions such as the area we focused on in this study, where complex
233 bathymetry and shoreline structure, and proximity to large islands, likely result in current
234 dynamics that are highly variable spatially and temporally.

235

236 **Trajectory results**

237 The sloughed *Cladophora* particles were released from the productive shallow areas
238 during the growing seasons, and their trajectory as determined by physical advection and
239 resuspension were predicted without algae aggregation and biological degradation considered.
240 The particle model indicated that only a small portion of particles was transported out of the
241 SLBE region (Fig. 5), implying the impacts of sloughed *Cladophora* on nutrient cycling,
242 energy flow, and shoreline conditions are largely confined at a regional/local scale. The
243 trajectory simulation results suggested that the majority of sloughed *Cladophora*, if not
244 washed up on the shoreline or beach, quickly deposited at nearby sites after sloughing
245 because of the sinking process (Fig. 5). Those *Cladophora* particles depositing at the shallow
246 nearshore sites could be easily resuspended to the water column due to relatively strong near
247 bottom currents. Differently, drifting *Cladophora* particles generally could not be resuspended
248 to the water column when they finally deposited to the mid-depth region (with a depth
249 between 20–50 m) unless significant upwelling and storm events occur. The mechanisms
250 driving *Cladophora* deposition are complex, and multiple factors including wind, temperature,

251 geomorphology and hydrodynamics may affect the deposition process. When and where
252 *Cladophora* deposition will occur, though attracted substantial attentions due to its ecosystem
253 consequences, is still difficult to predict and have been less reported till now. Observations
254 along the shoreline of Lake Michigan suggest that much drifting *Cladophora* finally ends up
255 on beaches (Riley et al., 2015).

256 We counted the *Cladophora* particles deposited at the bottom of the 20m-depth site (Fig.
257 2) within a radius of 500 m between June and August, and compared the count to the
258 thickness of the depositional mat recorded by the underwater time-lapse camera. It should be
259 noted that the number of particles counted within the specified area only qualitatively
260 represent the predictions of the thickness of *Cladophora* mats. The variability and temporal
261 trend of bottom particle numbers at the observation site were quite consistent with the
262 dynamics of the benthic mat (Fig. 6). The camera recorded an increasing trend of 30 cm
263 thickness per month, with shorter term deposition and resuspension events. The trajectory
264 model also predicted an increasing deposition during the growing season with abundant
265 sloughed *Cladophora*, and the model successfully captured the rapid deposition immediately
266 followed by resuspension and export in early August. Compared with the mat thickness
267 recorded by the camera in summer, the model generally predicted a relatively smooth
268 increasing trend with less fluctuations, possibly resulting from the simplifying assumptions of
269 no community aggregation or biological degradation, which would accelerate deposition and
270 enhance decaying, respectively.

271 The particle model applied a cohesive shoreline boundary configuration instead of a
272 reflective one, with the objective of assessing the potential for accumulation of detached
273 *Cladophora* along the shore. The trajectory model results demonstrated that the quantity of
274 particles attached along the shoreline displayed substantial variability (Fig. 6). In general, the
275 shoreline beaches adjacent to the shallow productive area are much more vulnerable to
276 *Cladophora* fouling with an overall large number of particles accumulated in summer. The
277 shoreline with high fouling risk is the Platte Bay area, which is adjacent to a large area of
278 submerged aquatic vegetation, which becomes trapped in the bay by the prevailing northward
279 alongshore current in summer (Fig. 6). By comparison, simulated shoreline fouling in
280 Sleeping Bear Bay and Good Harbor Bay were more moderate. Though the summer-time

281 northward currents would favor the accumulation of local *Cladophora* particles, the benthic
282 algal biomass density near these two bay areas was comparably lower (Fig. 5), which reduced
283 the releasing of *Cladophora* particles and the potential washing up onto the shorelines.

284

285 **Model limitations and future work**

286 In our Lagrangian trajectory model, the detached benthic algae were treated as passive
287 particles in the aquatic environments to track their transport and deposition sites. The model is
288 simplified in that it ignores certain important physical and biological processes including
289 aggregation, decaying and decomposition, which inevitably will result in discrepancies
290 between observed and simulated results. For example, a fixed sinking velocity and
291 resuspension threshold were applied in our model. However, these values can be expected to
292 vary with the size of algal aggregations after detaching. To account for the biological and
293 physical aggregation, size-dependent sinking rates were generally applied to model their
294 advection transport (Ackleh and Fitzpatrick, 1997). Laboratory experimental results showed
295 relatively higher resuspension thresholds for large-size macroalgae compared with small
296 species (Flindt et al., 2007). As expected, model sensitivity scenarios indicated the distance
297 between detachments sites and depositional sites becomes smaller if higher sinking velocities
298 and resuspension thresholds are used. Similarly, a constant releasing rate of particles at the
299 shallow nearshore regions was applied, and the spatiotemporal dynamics of the benthic
300 sloughing influenced by the variabilities of biomass distributions and bottom shear stress had
301 not been fully considered. In our study, initiation of sloughed *Cladophora* was hypothetically
302 from the very shallow sites where photosynthesis of these benthic algae is possible. The
303 accuracy of initial distributions could be improved with more in situ data and remote sensing
304 images. Some success in using optical parameters to identify in situ density of submerged
305 aquatic vegetation has been achieved in the Great Lakes (Shuchman et al., 2013; Brooks et al.,
306 2015). Meanwhile, dynamics of *Cladophora* growth has been successfully simulated in the
307 Great Lakes through comparisons to abundant field observations (Auer et al., 2010; Higgins
308 et al., 2005a). These biological models, if coupled with the hydrodynamic models (e.g.,
309 FVCOM) to better represent the spatiotemporal dynamics of *Cladophora* biomass at different
310 depths, could provide more accurate and dynamic *Cladophora* sloughing rates to the

311 trajectory transport model in this study. *Cladophora* decomposition will be important to
312 account for, in part because the decomposition process may determine the location and timing
313 of botulism toxin production, and also because it will determine the long-term fate of
314 sloughed *Cladophora*. For example, if significant amounts of sloughed *Cladophora* remain
315 intact late into the fall, when the lake becomes isothermal and storm events promote deep
316 mixing and horizontal transport, then a significant portion of the *Cladophora* that has been
317 deposited close to its original sloughing location may ultimately be transported further
318 offshore, possibly contributing energy to the offshore food web (Turschak et al., 2014).

319 While prediction of the timing and magnitude of shoreline stranding and in-lake
320 depositional events can be improved with model refinement, the results of this study help to
321 determine the spatial scale over which *Cladophora* sloughing, transport and deposition can be
322 expected to occur on time scales of weeks to months. This has important implications for
323 critical in-lake processes such as energy transport, nutrient dynamics, oxygen dynamics, and
324 avian botulism outbreaks. Coupled hydrodynamic-biogeochemical models have been
325 established and used to investigate nutrient cycling in the Great Lakes (Rowe et al., 2017;
326 Shen et al., 2020). Meanwhile, existing *Cladophora* (or submerged aquatic vegetation)
327 models appear to reliably simulate the direct response of their growth and mortality to the
328 nearshore temperature, light and phosphate levels (Tomlinson et al., 2010). These existing
329 model studies make it possible to establish a much broader
330 hydrodynamic-biogeochemical-*Cladophora* coupled model, in which, the interactions
331 between the physical, biogeochemical and vegetation parts could all be simulated in a short
332 time step, and the parameter configuration and forcing driver of each sub-module could be
333 updated quickly. For example, the temperature and nutrient concentrations from the
334 hydrodynamic-biogeochemical module could drive the *Cladophora* module. Meanwhile, the
335 biomass density of these benthic algae could be used dynamically to better represent the
336 bottom roughness and wave-current interaction scheme for the hydrodynamic model (Aleynik
337 et al., 2016). The development of such model could improve the accuracy of simulations in
338 their biomass dynamics, transport, response to external nutrient loading management as well
339 as the potential ecosystem risks at a lake-wide scale.

340

341 **Management implications**

342 The trajectory model indicates that, on the time scale of weeks to months, most of the
343 sloughed *Cladophora* within the SLBE region does not transport to the offshore, generally
344 settling at nearby mid-depth sites where benthic shear stress is weak. Hence the anoxic
345 conditions required for *C. botulinum* growth are more likely to occur at these mid-depth sites.
346 Meanwhile, the shoreline beach of the Platte Bay is more vulnerable to fouling by sloughed
347 *Cladophora* according to the model results, and special attention needs to be paid in this area
348 to maintain ecosystem health and recreational function. The SLBE region is an avian botulism
349 hotspot in Lake Michigan (Chipault et al., 2015; Chun et al., 2013), and if *Cladophora*
350 sloughing and decomposition is indeed a factor promoting the production of the botulism
351 toxin, the results presented here suggest that the unique set of features of this region,
352 including plentiful hard, shallow substrate, high areal concentrations of benthic algae, and
353 complex bathymetry that promotes the retention of sloughed algae, may explain why the
354 region has this distinction.

355 The depth averaged circulation along the SLBE shoreline in summer is traditionally
356 northward under the seasonal southwest winds (Beletsky and Schwab, 2001), and this
357 prevailing current prevents large portions of detached *Cladophora* from moving out of the
358 local bay area, leaving it to either be deposited at mid-depth sites or stranded on the shore.
359 These findings underscore the potential impact of localized *Cladophora* management actions
360 on *Cladophora* deposition in beach and nearshore waters at SLBE. The growth of *Cladophora*
361 in the Great Lakes is basically limited by light, temperature and phosphate (Tomlinson et al.,
362 2010). Favorable *Cladophora* growing conditions, including increased water clarity and light
363 availability are likely to persist for some time due to widespread dreissenid mussel
364 colonization in the broader lake. Nutrient limitation (phosphorus in specific) remains the most
365 viable way to restrict *Cladophora* growth and related fouling of nearshore and beach
366 environments. The phosphorus loading management since 1970s have successfully led to
367 lake-wide *Cladophora* biomass reduction, though the invasive benthic mussels reduced the
368 efficiency of such actions (Bootsma et al., 2015). In the more recent Great Lakes Water
369 Quality Protocol of 2012, developing phosphorus loading targets is recognized a key step to a
370 healthy lake ecosystem, particularly for the nearshore waters. Though invasive mussels were

371 supposed to be associated with the resurgence of benthic *Cladophora*, recent invasive mussel
372 control experiments on Good Harbor Reef resulted in shifts in benthic algal communities and
373 biomass, and may provide an alternative technique for managing localized growth and
374 deposition of *Cladophora* in the future (LimnoTech, 2020).

375

376 **Conclusions**

377 In this study, we applied a hydrodynamic and particle trajectory model to simulate the
378 transport of sloughed *Cladophora* in the SLBE area. The hydrodynamic model well
379 reproduced the physical features in the study area, including a relatively small RMSE of
380 0.6 °C between simulated and observed surface water temperature, and comparable near-bottom
381 current speeds (1.6 vs 1.4 cm s⁻¹). The trajectory model qualitatively predicted the thickness
382 dynamics of depositional mats, with temporal patterns fairly consistent with those recorded by
383 the time lapse camera (~30 cm thickness increase per month). Our model results revealed that
384 the sloughed *Cladophora* generally deposited at nearby mid-depth regions (20-50 m) after
385 detached from their growing sites. The southern shoreline beaches, particularly around the
386 Platte Bay, was demonstrated vulnerable to the fouling of decayed *Cladophora*. Our study is a
387 first trial to simulate the trajectory of detached *Cladophora*, and could inform the regional
388 ecosystem management.

389

390 **Declaration of competing interest**

391 The authors declare that they have no known competing financial interests or personal
392 relationships that could have appeared to influence the work reported in this paper.

393

394 **Acknowledgement**

395 This material is based upon work supported by the Wisconsin Sea Grant under Project
396 No. R/HEC-17 and R/HEC-36, the National Science Foundation under Grant No. 1658390,
397 and the U.S. EPA Great Lakes Restoration Initiative, via a cooperative agreement with the
398 National Park Service.

399

400 **References**

401 Ackleh, A.S. and Fitzpatrick, B.G., 1997. Modeling aggregation and growth processes in an algal
402 population model: analysis and computations. *Journal of Mathematical Biology*, 35(4),
403 pp.480-502.

404 Aleynik, D., Dale, A.C., Porter, M. and Davidson, K., 2016. A high resolution hydrodynamic model
405 system suitable for novel harmful algal bloom modelling in areas of complex coastline and
406 topography. *Harmful algae*, 53, pp.102-117.

407 Anderson, E.J., Bechle, A.J., Wu, C.H., Schwab, D.J., Mann, G.E. and Lombardy, K.A., 2015.
408 Reconstruction of a meteotsunami in Lake Erie on 27 May 2012: Roles of atmospheric
409 conditions on hydrodynamic response in enclosed basins. *Journal of Geophysical Research:*
410 *Oceans*, 120(12), pp.8020-8038.

411 Auer, M.T., Tomlinson, L.M., Higgins, S.N., Malkin, S.Y., Howell, E.T. and Bootsma, H.A., 2010.
412 Great Lakes Cladophora in the 21st century: same algae—different ecosystem. *Journal of Great*
413 *Lakes Research*, 36(2), pp.248-255.

414 Auer, M.T., McDonald, C.P., Kuczynski, A., Huang, C. and Xue, P., 2021. Management of the
415 Phosphorus–Cladophora Dynamic at a Site on Lake Ontario Using a Multi-Module Bioavailable P
416 Model. *Water*, 13(3), p.375.

417 Bai, X., Wang, J., Schwab, D.J., Yang, Y., Luo, L., Leshkevich, G.A. and Liu, S., 2013. Modeling
418 1993–2008 climatology of seasonal general circulation and thermal structure in the Great Lakes
419 using FVCOM. *Ocean Modelling*, 65, pp.40-63.

420 Beletsky, D. and Schwab, D.J., 2001. Modeling circulation and thermal structure in Lake Michigan:
421 Annual cycle and interannual variability. *Journal of Geophysical Research: Oceans*, 106(C9),
422 pp.19745-19771.

423 Beletsky, D., Mason, D.M., Schwab, D.J., Rutherford, E.S., Janssen, J., Clapp, D.F. and Dettmers, J.M.,
424 2007. Biophysical model of larval yellow perch advection and settlement in Lake
425 Michigan. *Journal of Great Lakes Research*, 33(4), pp.842-866.

426 Beletsky, D., Hawley, N. and Rao, Y.R., 2013. Modeling summer circulation and thermal structure of
427 Lake Erie. *Journal of Geophysical Research: Oceans*, 118(11), pp.6238-6252.

428 Bootsma, H.A., Young, E.B. and Berges, J.A., 2004. Temporal and spatial patterns of Cladophora
429 biomass and nutrient stoichiometry in Lake Michigan. *Cladophora research and management in*
430 *the Great Lakes*. University of Wisconsin-Milwaukee.

431 Bootsma, H.A., Liao, Q., 2013. Nutrient cycling by dreissenid mussels: controlling factors and
432 ecosystem response. In: Nalepa, T.F., Schloesser, D.W. (Eds.), *Quagga and ZebraMussels: Biology,*
433 *Impacts and Control*, 2nd ed. CRC Press, Boca Raton, FL, pp. 555–574

434 Bootsma, H.A., M.D. Rowe, C.N. Brooks, and H.A. Vanderploeg. 2015. Commentary: The need for
435 model development related to *Cladophora* and nutrient management in Lake Michigan. *Journal of*
436 *Great Lakes Research*, 41 (Suppl. 3), pp.7-15.

437 Brooks, C., Grimm, A., Shuchman, R., Sayers, M. and Jessee, N., 2015. A satellite-based
438 multi-temporal assessment of the extent of nuisance Cladophora and related submerged aquatic
439 vegetation for the Laurentian Great Lakes. *Remote Sensing of Environment*, 157, pp.58-71.

440 Byappanahalli, M.N. and Whitman, R.L., 2009. Clostridium botulinum type E occurs and grows in the
441 alga Cladophora glomerata. *Canadian Journal of Fisheries and Aquatic Sciences*, 66(6),
442 pp.879-882.

443 Chapra, S.C., Sonzogni, W.C., 1979. Great Lakes total phosphorus budget for the mid- 1970s. *J. Water*
444 *Pollut. Control Fed.* 2524–33.

445 Chen, C., Ji, R., Schwab, D.J., Beletsky, D., Fahnenstiel, G.L., Jiang, M., Johengen, T.H., Vanderploeg,
446 H., Eadie, B., Budd, J.W. and Bundy, M.H., 2002. A model study of the coupled biological and
447 physical dynamics in Lake Michigan. *Ecological modelling*, 152(2-3), pp.145-168.

448 Chipault, J.G., White, C.L., Blehert, D.S., Jennings, S.K. and Strom, S.M., 2015. Avian botulism type E
449 in waterbirds of Lake Michigan, 2010–2013. *Journal of Great Lakes Research*, 41(2), pp.659-664.

450 Chun, C.L., Ochsner, U., Byappanahalli, M.N., Whitman, R.L., Tepp, W.H., Lin, G., Johnson, E.A.,
451 Peller, J. and Sadowsky, M.J., 2013. Association of toxin-producing *Clostridium botulinum* with
452 the macroalga *Cladophora* in the Great Lakes. *Environmental science & technology*, 47(6),
453 pp.2587-2594.

454 Chun, C.L., Peller, J.R., Shively, D., Byappanahalli, M.N., Whitman, R.L., Staley, C., Zhang, Q., Ishii,
455 S. and Sadowsky, M.J., 2017. Virulence and biodegradation potential of dynamic microbial
456 communities associated with decaying *Cladophora* in Great Lakes. *Science of the Total
457 Environment*, 574, pp.872-880.

458 Dayton, A.I., Auer, M.T. and Atkinson, J.F., 2014. *Cladophora*, mass transport, and the nearshore
459 phosphorus shunt. *Journal of Great Lakes Research*, 40(3), pp.790-799.

460 Flindt, M.R., Pedersen, C.B., Amos, C.L., Levy, A., Bergamasco, A. and Friend, P.L., 2007. Transport,
461 sloughing and settling rates of estuarine macrophytes: Mechanisms and ecological
462 implications. *Continental Shelf Research*, 27(8), pp.1096-1103.

463 Gill, D., Rowe, M. and Joshi, S.J., 2018. Fishing in greener waters: understanding the impact of
464 harmful algal blooms on Lake Erie anglers and the potential for adoption of a forecast
465 model. *Journal of environmental management*, 227, pp.248-255.

466 Hecky, R.E., Smith, R.E., Barton, D.R., Guildford, S.J., Taylor, W.D., Charlton, M.N. and Howell, T.,
467 2004. The nearshore phosphorus shunt: a consequence of ecosystem engineering by dreissenids in
468 the Laurentian Great Lakes. *Canadian Journal of Fisheries and Aquatic Sciences*, 61(7),
469 pp.1285-1293.

470 Higgins, S.N., Howell, E.T., Hecky, R.E., Guildford, S.J. and Smith, R.E., 2005a. The wall of green:
471 the status of *Cladophora glomerata* on the northern shores of Lake Erie's eastern basin, 1995–
472 2002. *Journal of Great Lakes Research*, 31(4), pp.547-563.

473 Higgins, S.N., Hecky, R.E., and Guildford, S.J. 2005b. Modeling the growth, biomass, and tissue
474 phosphorus concentration of *Cladophora glomerata* in eastern Lake Erie: Model description and
475 field testing. *Journal of Great Lakes Research*, 31, pp. 439-455.

476 Higgins, S.N., Malkin, S.Y., Todd Howell, E., Guildford, S.J., Campbell, L., Hiriart-Baer, V. and Hecky,
477 R.E., 2008. An ecological review of *Cladophora glomerata* (Chlorophyta) in the Laurentian Great
478 Lakes 1. *Journal of Phycology*, 44(4), pp.839-854.

479 Huret, M., Runge, J.A., Chen, C., Cowles, G., Xu, Q. and Pringle, J.M., 2007. Dispersal modeling of
480 fish early life stages: sensitivity with application to Atlantic cod in the western Gulf of
481 Maine. *Marine Ecology Progress Series*, 347, pp.261-274.

482 Kuczynski, A., Auer, M.T., Brooks, C.N. and Grimm, A.G., 2016. The *Cladophora* resurgence in Lake
483 Ontario: characterization and implications for management. *Canadian journal of fisheries and
484 aquatic sciences*, 73(6), pp.999-1013.

485 Lenzi, M., Salvaterra, G., Gennaro, P., Mercatali, I., Persia, E., Porrello, S. and Sorce, C., 2015. A new
486 approach to macroalgal bloom control in eutrophic, shallow-water, coastal areas. *Journal of
487 environmental management*, 150, pp.456-465.

488 LimnoTech 2020. Good Harbor Bay dreissenid mussel control demonstration project. Final Project

489 Report prepared for Great Lakes Commission and Invasive Mussel Collaborative partners. 84 pp.
490 Malkin, S.Y., Guildford, S.J. and Hecky, R.E., 2008. Modeling the growth response of *Cladophora* in a
491 Laurentian Great Lake to the exotic invader *Dreissena* and to lake warming. *Limnology and*
492 *Oceanography*, 53(3), pp.1111-1124.
493 Mathai, P.P., Dunn, H.M., Magnone, P., Zhang, Q., Ishii, S., Chun, C.L. and Sadowsky, M.J., 2019.
494 Association between submerged aquatic vegetation and elevated levels of *Escherichia coli* and
495 potential bacterial pathogens in freshwater lakes. *Science of the Total Environment*, 657,
496 pp.319-324.
497 Princé, K., Chipault, J.G., White, C.L., and Zuckerberg, B. 2017. Environmental conditions
498 synchronize waterbird mortality events in the Great Lakes. *Journal of Applied Ecology*, 55(3), pp.
499 1327-1338.
500 Przybyla-Kelly, K., Nevers, M.B., Breitenbach, C. and Whitman, R.L., 2013. Recreational water
501 quality response to a filtering barrier at a Great Lakes beach. *Journal of environmental*
502 *management*, 129, pp.635-641.
503 Riley, S.C., Tucker, T.R., Adams, J.V., Fogarty, L.R. and Lafrancois, B.M., 2015. Factors associated
504 with the deposition of *Cladophora* on Lake Michigan beaches in 2012. *Journal of Great Lakes*
505 *Research*, 41(4), pp.1094-1105.
506 Rowe, M.D., Anderson, E.J., Wynne, T.T., Stumpf, R.P., Fanslow, D.L., Kijanka, K., Vanderploeg, H.A.,
507 Strickler, J.R. and Davis, T.W., 2016. Vertical distribution of buoyant *Microcystis* blooms in a
508 Lagrangian particle tracking model for short-term forecasts in Lake Erie. *Journal of Geophysical*
509 *Research: Oceans*, 121(7), pp.5296-5314.
510 Rowe, M.D., Anderson, E.J., Vanderploeg, H.A., Pothoven, S.A., Elgin, A.K., Wang, J. and Yousef, F.,
511 2017. Influence of invasive quagga mussels, phosphorus loads, and climate on spatial and
512 temporal patterns of productivity in Lake Michigan: A biophysical modeling study. *Limnology and*
513 *Oceanography*, 62(6), pp.2629-2649.
514 Shen, C., Liao, Q., Bootsma, H.A., Troy, C.D. and Cannon, D., 2018. Regulation of plankton and
515 nutrient dynamics by profundal quagga mussels in Lake Michigan: a one-dimensional
516 model. *Hydrobiologia*, 815(1), pp.47-63.
517 Shen, C., Liao, Q. and Bootsma, H.A., 2020. Modelling the influence of invasive mussels on
518 phosphorus cycling in Lake Michigan. *Ecological Modelling*, 416, p.108920.
519 Shuchman, R.A., Sayers, M.J. and Brooks, C.N., 2013. Mapping and monitoring the extent of
520 submerged aquatic vegetation in the Laurentian Great Lakes with multi-scale satellite remote
521 sensing. *Journal of Great Lakes Research*, 39, pp.78-89.
522 Tomlinson, L.M., Auer, M.T., Bootsma, H.A. and Owens, E.M., 2010. The Great Lakes *Cladophora*
523 model: development, testing, and application to Lake Michigan. *Journal of Great Lakes*
524 *Research*, 36(2), pp.287-297.
525 Turschak, B.A., Bunnell, D., Czesny, S., Höök, T.O., Janssen, J., Warner, D. and Bootsma, H.A., 2014.
526 Nearshore energy subsidies support Lake Michigan fishes and invertebrates following major
527 changes in food web structure. *Ecology*, 95(5), pp.1243-1252.
528 Tyner, E., 2013. Nearshore benthic oxygen dynamics in Lake Michigan (MS Thesis, University of
529 Wisconsin-Milwaukee).
530 Waples, J.T., Bootsma, H.A. and Klump, J.V., 2017. How are coastal benthos fed? *Limnology and*
531 *Oceanography Letters*, 2(1), pp.18-28.
532 Xue, P., Schwab, D.J. and Hu, S., 2015. An investigation of the thermal response to meteorological

533 forcing in a hydrodynamic model of Lake Superior. *Journal of Geophysical Research:*
534 *Oceans*, 120(7), pp.5233-5253.
535

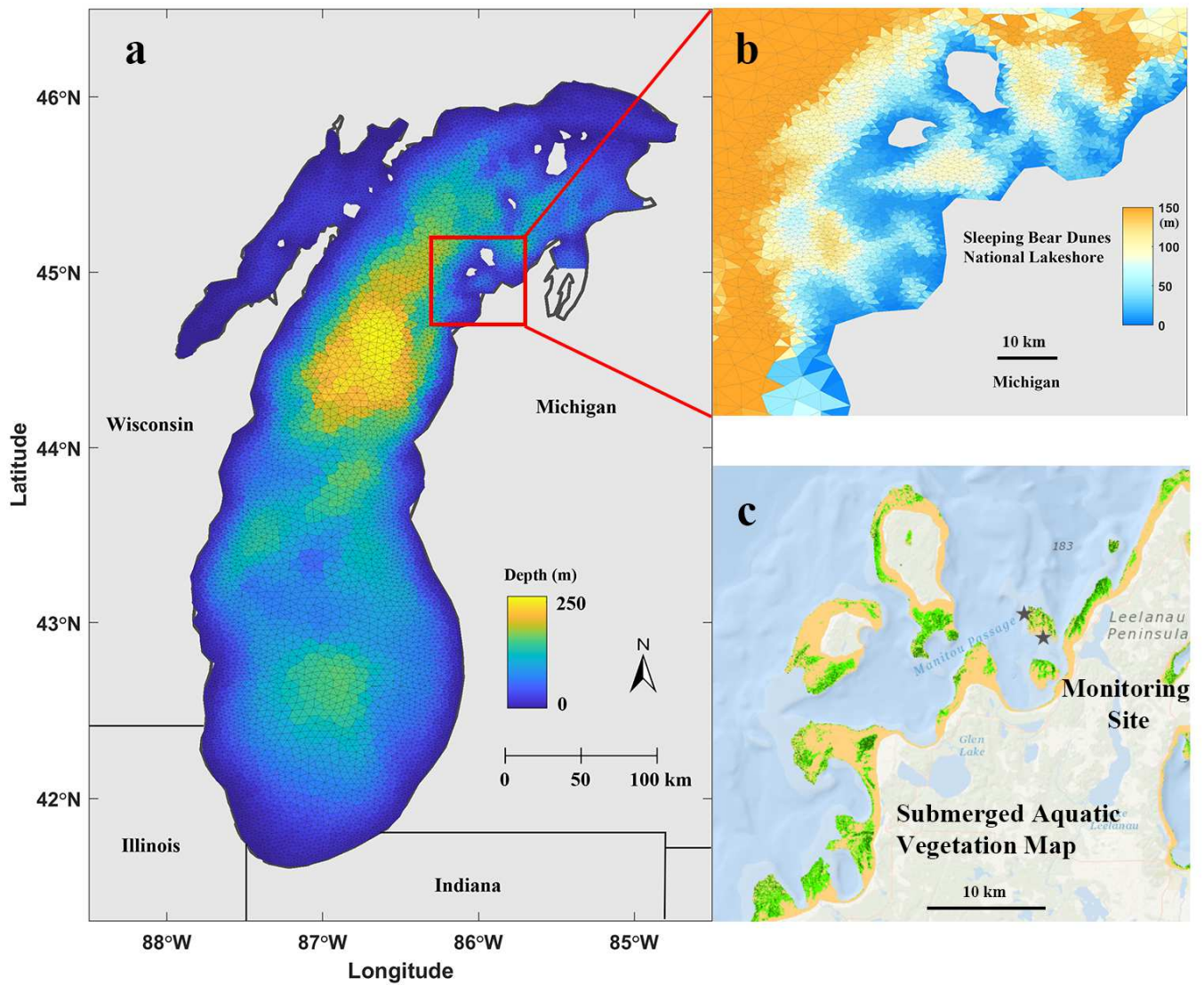


Fig. 1 (a) Bathymetry and model mesh grids of Lake Michigan. (b) The nested high-resolution grids at the Sleeping Bear Dunes National Lakeshore area (c) Submerged aquatic vegetation distribution within the region, as determined with satellite imagery (Brooks et al., 2015).

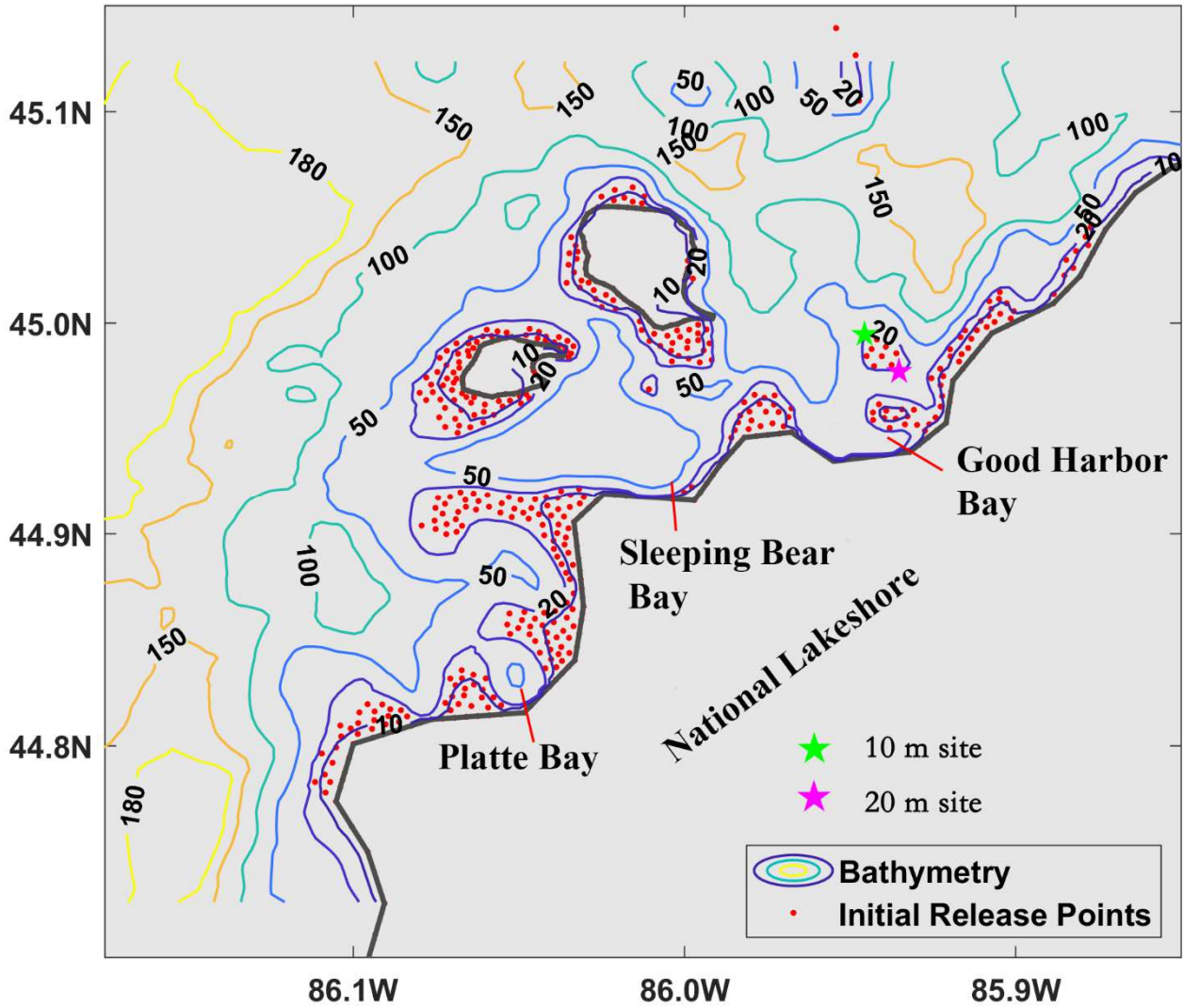


Fig. 2 Detailed bathymetry map of the study area. Red dots represent the growth and detaching sites of *Cladophora*, pink star represents the 20 m field observational site, and green star represents the 10 m site.

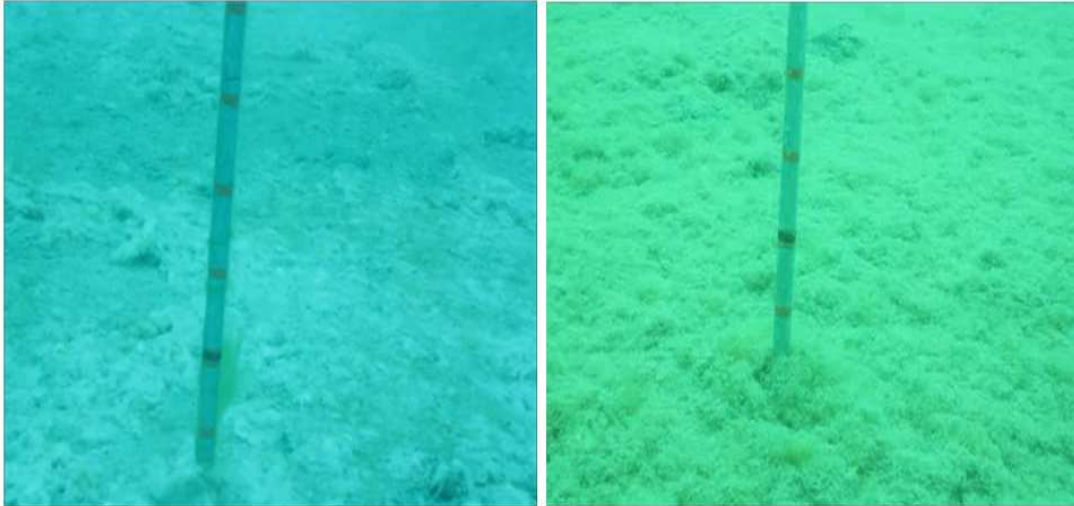


Fig. 3 Time lapse images of bed thickness at the Good Harbor Bay depositional site (20m depth). The vertical measuring stick is used to record the thickness of the deposition mats. Left: June 10. Right: August 10.

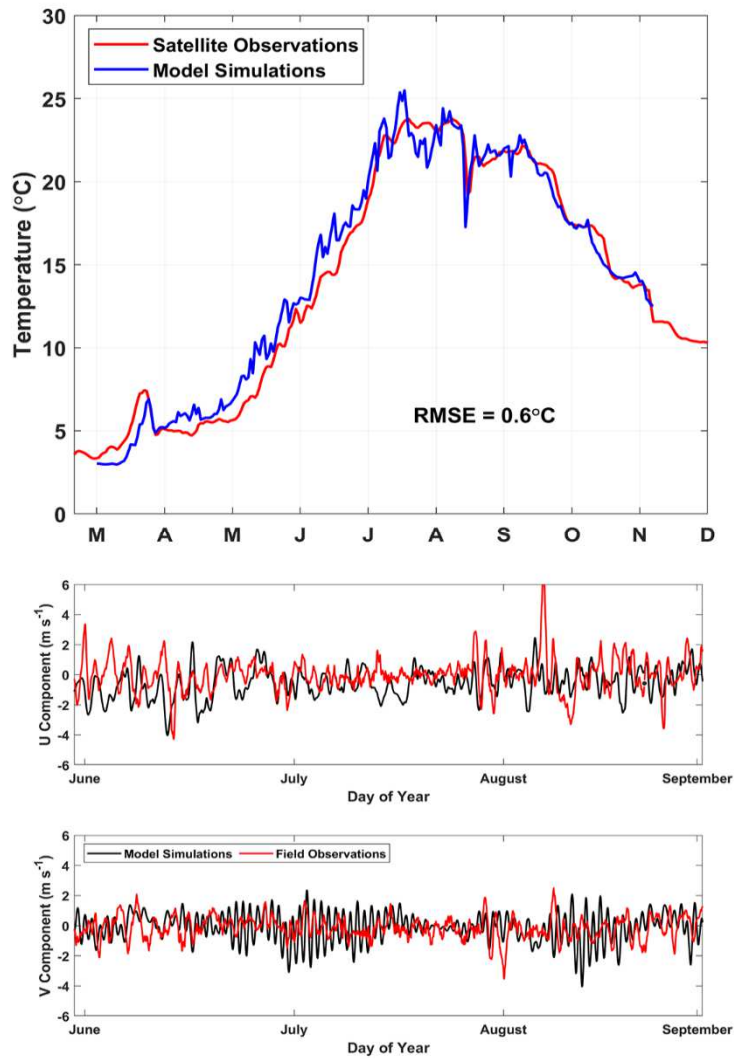


Fig. 4. (up) Comparisons of simulated and satellite-derived surface water temperatures in the SLBE Good Harbor Bay region. (bottom) Comparisons of simulated and measured (ADCP) northern and eastern near-bottom current velocity components at the Good Harbor Bay site (10m-depth site).

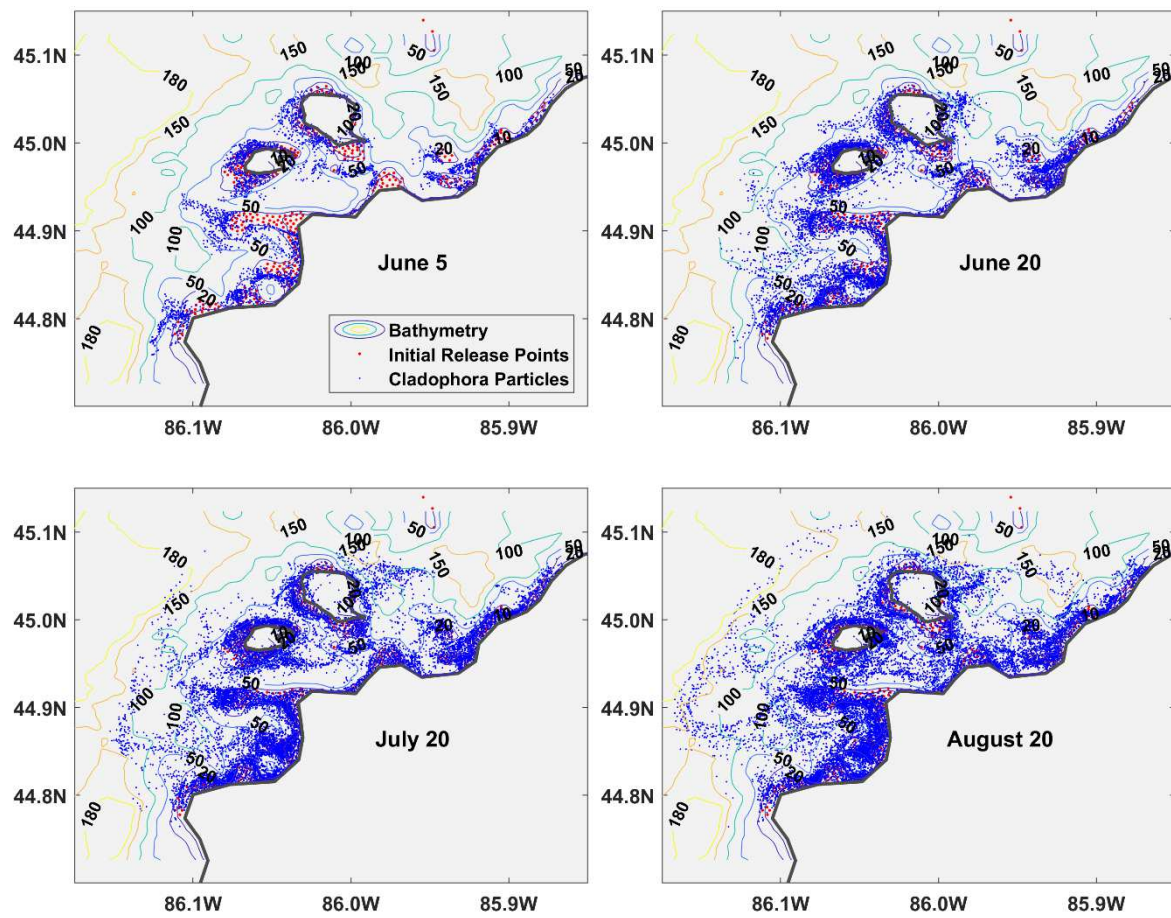


Fig. 5 Simulated distribution maps of detached *Cladophora* particles within the national lakeshore in June 5th, June 20th, July 20th and August 20th.

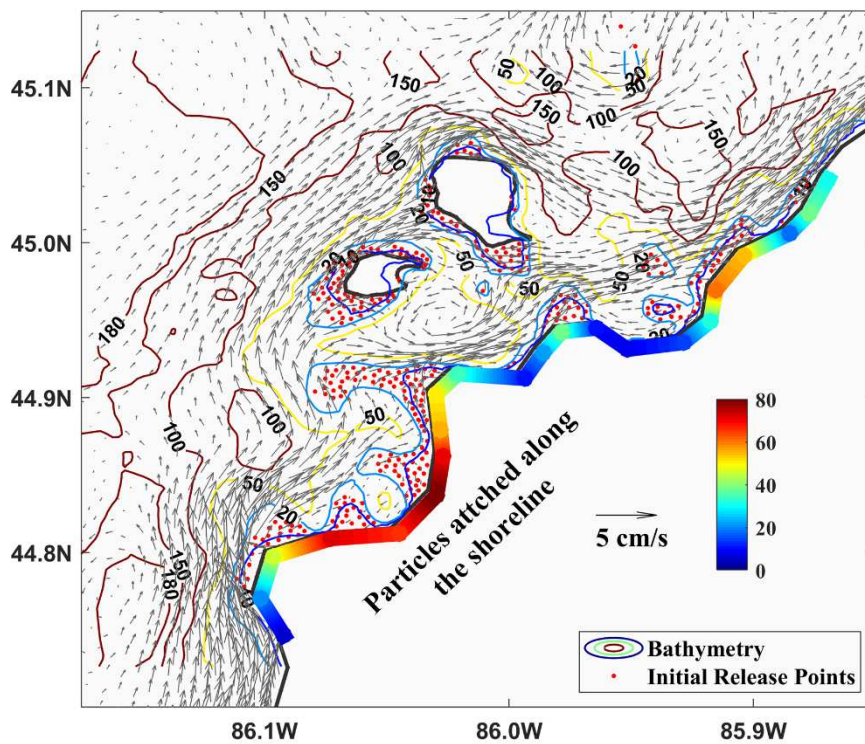
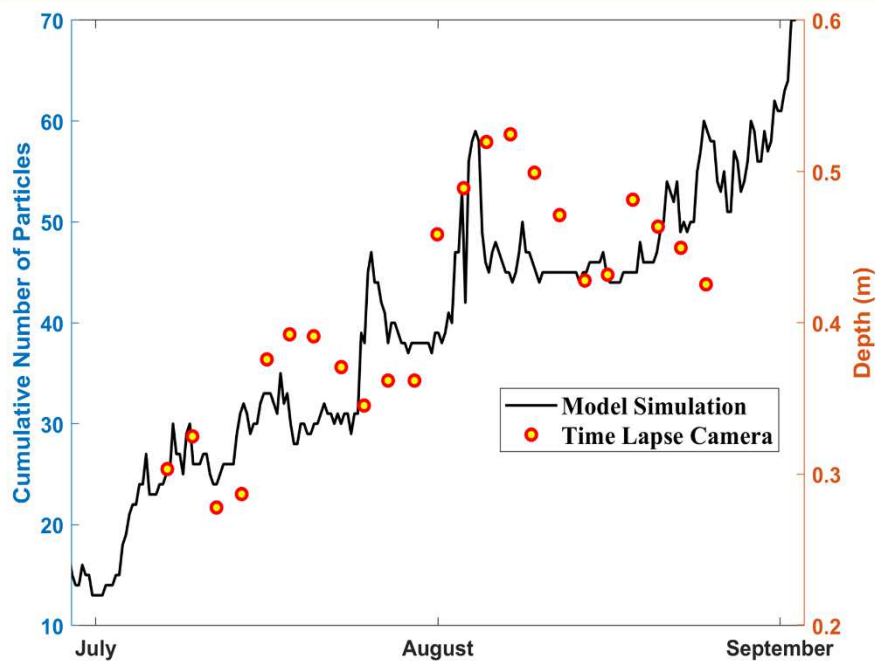


Fig. 6. (up) Comparisons between counted particles from model simulations and deposition mats thickness recorded by the underwater camera. (bottom) Depth averaged currents of the study area in summer and accumulated particles along the shoreline beaches.

